Supporting Information for

Organometallic Ni(II), Ni(III), and Ni(IV) Complexes Relevant to Carbon-Carbon and Carbon-Oxygen Bond Formation Reactions

Carla Magallon,[a] Leonel Griego,[b] Daniel Hu,[b] Anna Company,*[,a] Xavi Ribas,*[,a] Liviu M. Mirica*[,b]

[a]Institut de Química Computacional i Catàlisi (IQCC) and Departament de Química, Universitat de Girona, Campus Montilivi, Girona, E-17003, Catalonia, Spain
[b]Department of Chemistry, University of Illinois at Urbana-Champaign, 600 S. Mathews Avenue, Urbana, Illinois 61801, USA.

*Corresponding author: mirica@illinois.edu

Table of contents

1. General considerations

Materials and methods

All manipulations were carried out under a nitrogen atmosphere (with O_2 and H_2O concentrations < 1 ppm) using standard Schlenk and glove box techniques, unless otherwise indicated. All reagents for which synthesis is not given are commercially available from Sigma Aldrich, Acros, or STREM and were used as received without further purification. Solvents were purified prior to use by passing through a column of activated molecular sieves using an MBRAUN SPS. The **$PyNMe_3$** ligand[1, 2] and the $(Py)_2Ni^{II}$(cycloneophyl)[3] precursor were prepared according to previously reported protocols in the literature. Other abbreviations used throughout the paper and supporting information: ferrocenium hexafluorophosphate ($FcPF_6$), nitrosonium hexafluorophosphate ($NOPF_6$), nitrosonium hexafluoroantimonate ($NOSbF_6$), 1-Fluoro-2,4,6-trimethylpyridinium triflate (NFTPT), hydrogen peroxide (H_2O_2), *tert*-butyl hydroperoxide ($^tBuO_2H$), xenon difluoride (XeF_2) and (diacetoxyiodo)benzene ($PhI(OAc)_2$).

NMR data concerning product identity were collected with a Bruker 500 spectometer (500 MHz). Chemical shifts are reported in ppm and referenced to residual solvent resonance peaks. Abbreviations for the multiplicity of NMR signals are s (singlet), d (doublet), dd (doublet of doublets), t (triplet), m (multiplet). All NMR experiments were recorded and processed using standard parameters and no more details are given, unless otherwise stated. EPR spectra were recorded using a Bruker 10" EMXPlus X-band Continuous Wave EPR spectrometer at 77 K. EPR spectra simulation and analysis were performed using Bruker WINEPR SimFonia program, version 1.25. GC-MS data was collected using an Agilent 7890B GC Series System and an Agilent 5977B Mass Selective Detector. High resolution mass spectra (HRMS) were recorded on a Bruker MicrOTOF-Q IITM instrument using ESI as ionization source or CMS (cryospray ionization, for low temperature experiments) at Serveis Tècnics University of Girona. Samples were introduced into the mass spectrometer ion source by direct infusion and were externally calibrated using sodium triflate. The instrument was operated in the positive ion

mode. Electrochemical-grade electrolytes from Fluka were used as the supporting electrolyte for electrochemical measurements. Cyclic voltammetry experiments were performed with a BASi EC Epsilon electrochemical workstation or a CHI 660D Electrochemical Analyzer. The electrochemical measurements were taken in a glove box under nitrogen. A glassy carbon disk electrode (d = 1.6 mm) was used as the working electrode for cyclic voltammetry. The auxiliary electrode was a Pt wire for cyclic voltammetry measurements. The non-aqueous references electrode used was a silver wire. The reference electrodes were calibrated against ferrocene (Fc). UV-vis spectroscopy was performed with an Agilent 8453 UV-vis spectrophotometer with 1 cm quartz cells. Low temperature control was achieved with a cryostat from Unisoku Scientific Instruments, Japan. Elemental analysis was carried out by the Microanalysis Laboratory at UIUC using an Exeter Analytical - Model CE440 CHN Analyzer.

2. Synthesis of [(PyNMe$_3$)Ni^{II}(PhF)(Br)] and 1-Br

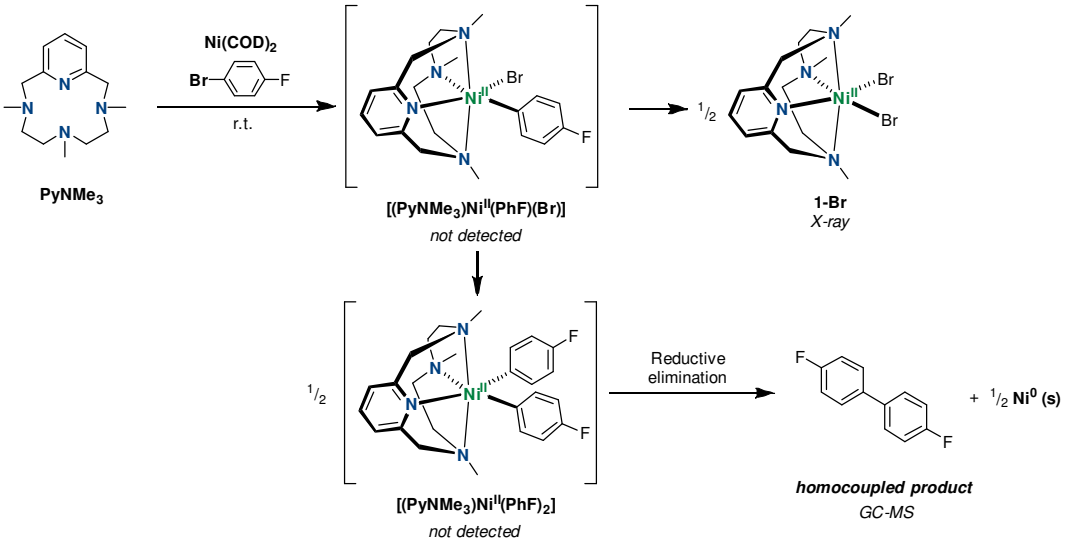

Scheme S1. Attempt to synthesize complex [(**PyNMe$_3$**)Ni^{II}(**PhF**)(**Br**)].

In a N_2-filled glovebox, **PyNMe$_3$** (38mg, 0.15 mmols) and Ni(COD)$_2$ (42.1 mg, 0.15 mmols) were dissolved in ~3 mL of 4-**f**luorobromobenzene. The mixture was stirred for 4 hours at room temperature, and a green solid formed with specs of a black solid. The mixture was collected and washed with diethylether to remove excess solvent and ligand. [(PyNMe$_3$)Ni^{II}(Br)$_2$] (1-Br) and Ni(0) (64.9 mg, 0.13 mmol, 88% yield).

X-ray quality crystals were obtained from the slow diethylether vapor diffusion over a concentrated solution of the complex in MeCN at -35 ºC. The solid-state structure revealed **1-Br**. In addition, the reaction solution contained homocoupled product 4,4-difluorobiphenyl, detected via GC-MS.

3. Synthesis of 1-Cl and [(PyNMe$_3$)Ni^{II}(Me)$_2$]

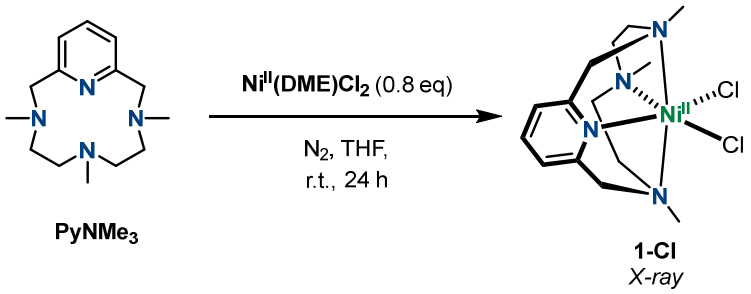

Scheme S2. Synthesis of **1-Cl**.

In the glovebox, **PyNMe$_3$** (29.2 mg, 0.12 mmol) was dissolved in THF (2 mL). Afterwards Ni^{II}(DME)Cl$_2$ (20.0 mg, 0.09 mmol) was added directly as a solid and the mixture was stirred for 24 hours. After that, the formation of a green suspension was observed. Then the suspension was crashed out with diethyl ether, filtered and dried under vacuum obtaining 28.5 mg of a green solid corresponding to [**(PyNMe$_3$)Ni^{II} (Cl)$_2$**], **1-Cl** (0.08 mmol, 85% yield). X-ray quality crystals were obtained after redissolving the green solid in MeCN and by slow diethyl ether diffusion at room temperature.

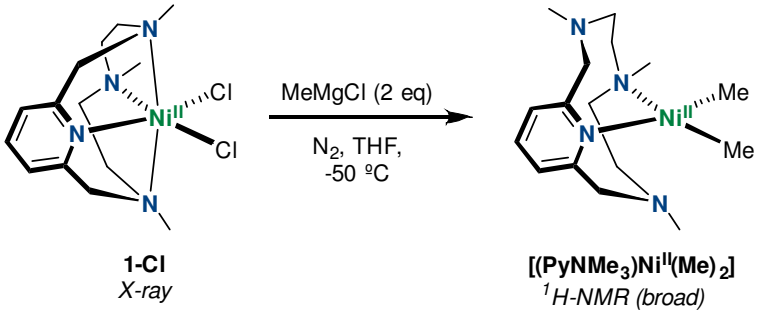

Scheme S3. Attempt to synthesize **[(PyNMe3)NiII(PhF)(Br)].**

In a N$_2$-filled glovebox, **1-Cl** (35.5 mg, 0.09 mmol) was suspended in THF and cooled down to -50 ºC. Then 66 µL of a 3M solution of cold MeMgCl in THF was added dropwise and upon addition of the MeMgCl a color change from green to red was observed. The suspension was left stirring for 1 hour at -50 ºC in the glovebox freezer and then the solvent was evaporated under vacuum at -50 ºC. After that toluene was added to precipitate the magnesium salts and the mixture

(orange) was filtered twice through a celite® pad and once through a kim-wipe. The solvent was removed under vacuum and the orange-black solid was dissolved in benzene-d_6 to take ^{1}H NMR at r.t of the putative **[(PyNMe$_3$)Ni^{II}(Me)$_2$]** formed.

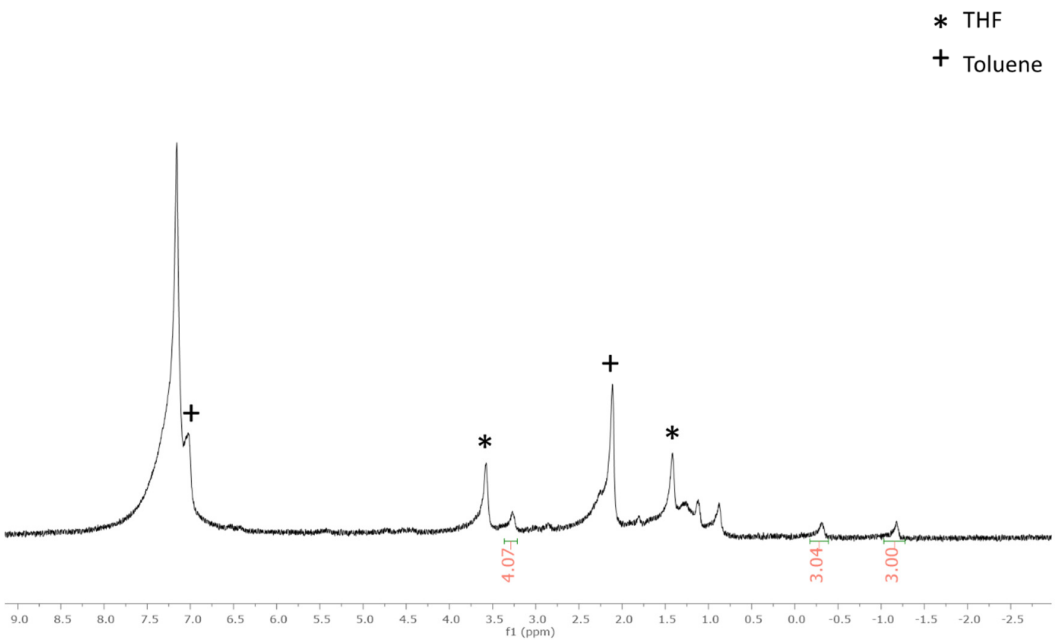

Figure S1. ^{1}H NMR (500 MHz, C_6D_6, 298 K) spectrum of the putative **[(PyNMe$_3$)Ni^{II}(Me)$_2$]** (* corresponds to THF solvent peaks, and $^+$ corresponds to toluene solvent peaks).

4. Synthesis of [(PyNMe$_3$)Ni(cycloneophyl)]

4.1. Preparation of [(PyNMe$_3$)Ni^{II}(cycl), 2

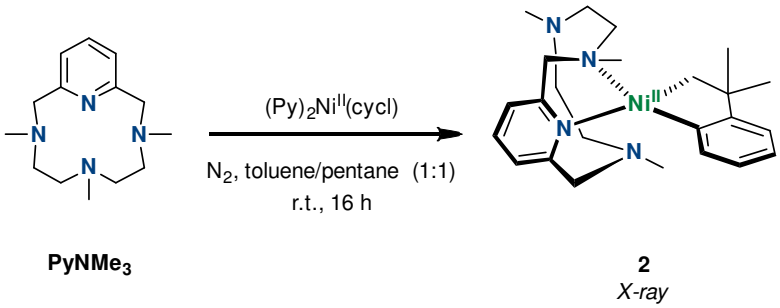

Scheme S4. Synthesis of **2**.

In the glovebox, **PyNMe$_3$** (70.9 mg, 0.28 mmol) and (Py)$_2$Ni^{II}(cycl) (65.2 mg, 0.19 mmols) were dissolved in 3 mL toluene/pentane (1:1). The mixture was stirred for

16 hours at room temperature. After that the orange-red suspension was dried under vacuum. Then the orange solid obtained was washed with diethyl ether to remove any ligand in excess. The suspension was filtered and the solid was redissolved in the minimum amount of THF. Slow pentane diffusion over a concentrated solution of the complex in THF at -35 ºC afforded orange crystals corresponding to [(**PyNMe$_3$**)**Ni^{II}(cycl)**], **2** (58.3 mg, 0.13 mmol, 71 % yield).

^{1}H NMR (500 MHz, C_6D_6, 298 K) δ (ppm): 7.19-7.10 (m, 2H, **C**), 6.93 (m, 1H, **C**), 6.86 (m, 1H, **F**), 6.54 (b, 1H, **C**), 6.50 (m, 2H, **F**), 4.82 (d, 2H, **G**), 3.00 (b, 2H, **E**), 2.87 (b, 2H, **G**), 2.44 (b, 2H, **E**), 2.22 (s, 3H, **D**), 2.07 (s, 6H, **D**), 1.90 (s, 6H, **B**), 1.85 (b, 3H,) 1.71 (b, 2H, **E**), 1.35 (s, 2H, **A**); Ligand Impurities: 6.78, 3.69, 3.56, 2.71, 2.60, 2.33, 2.18

^{13}C NMR (500 MHz, C_6D_6, 298 K), δ (ppm): 169.5 (**c**), 159.8 (**f**), 159.0 (**c**), 157.8 (**f**), 136.7 (**c**), 136.1 (**f**), 134.5 (**f**), 122.6 (**c**), 121.8 (**c**), 121.4 (**f**), 120.8 (**c**), 65.0 (**g**), 56.5 (**e**), 55.9 (**e**), 47.8 (**h**), 47.1 (**d**), 44.4 (**d**), 40.7 (**a**), 34.2 (**b**) ; Ligand Impurities: 62.5, 52.1, 51.4, 45.1, 44.1

EA: calcd. for $C_{24}H_{36}N_4Ni$, C 65.62, N 12.75, H 8.26 %; exp. C 66.01, N 12.83, H 8.37 %.

UV-vis(233 K): λ_{max} = 460 nm (ε = 880 $M^{-1}cm^{-1}$)

4.2. Preparation of [(PyNMe$_3$)Ni^{III}(cycl)](PF$_6$), 3

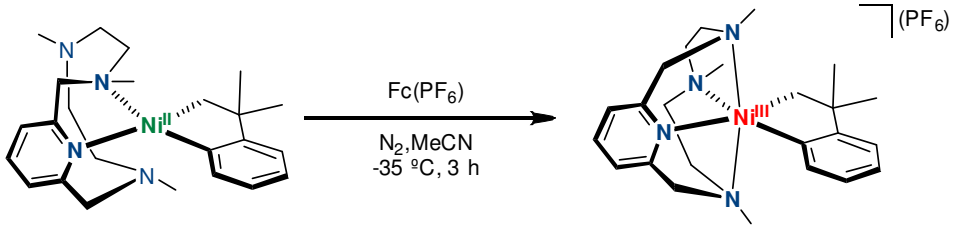

2 **3** *X-ray*

Scheme S5. Synthesis of **3**.

In the glovebox, complex **2** (23.4 mg, 0.05 mmol) was dissolved in 2 mL of MeCN and Fc(PF$_6$) (17.6 mg, 0.05 mmols) was added at -50 ºC. The mixture was stirred for 3 hours at -35 ºC. After that the mixture was concentrated under vacuum. X-ray quality crystals were obtained after a few days of storage of a concentrated solution

in MeCN at -35 ºC corresponding to **[(PyNMe$_3$)Ni^{III}(cycl)](PF$_6$), 3** (21.3 mg mg, 0.04 mmol, 73 % yield)

HR-CMS-MS (233 K): calcd. for $C_{24}H_{36}N_4Ni^+$ $[M\text{-}PF_6]^+$ 438.2288; exp 438.2289.

EPR $g_z = 2.235$; $g_y = 2.207$; $g_z = 2.016$, $A_{2N} = 13.7$ G

EA: calcd. for $C_{24}H_{36}N_4NiPF_6 \cdot 0.6(CH_3CN)$, C 48.53, N 10.58, H 6.26 %; exp. C 48.22, N 10.47, H 6.17 %.

UV-vis(233 K): λ_{max} = 510 nm (ε = 300 $M^{-1}cm^{-1}$)

4.3. NMR scale preparation of [(PyNMe$_3$)Ni^{IV}(cycloneophyl)](SbF$_6$)$_2$, 4

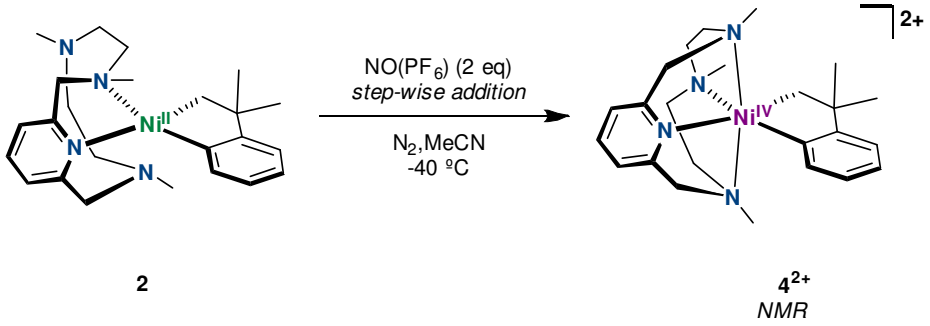

2 **4^{2+}** *NMR*

Scheme S6. NMR-scale synthesis of **4**.

In the glovebox, complex **2** (6.0 mg, 0.01 mmol) was dissolved in 200 µL CD_3CN, placed in an NMR tube and sealed with a septum cap. A separate solution of $NO(PF_6)$ (3.5 mg, 0.02 mmols) in 200 µL of CD_3CN was added at -40 ºC in a stepwise fashion. The first equivalent of oxidant was added and quickly mixed in the NMR tube to get a pink-red paramagnetic solution. The second equivalent of oxidant was then added and mixed to obtain a dark orange diamagnetic solution corresponding to **[(PyNMe$_3$)Ni^{IV}(cycl)](PF$_6$)$_2$, 4**.

^{1}H NMR (500 MHz, CD_3CN, 238 K), δ (ppm): 8.38 (b, 1H, **L**), 7.78 (b, 2H, **K**), 7.14-7.05 (d, 3H, **B,C,D**), 6.70 (b, 1H, **A**), 5.25 (s, 2H, **F**), 3.70-2.86 (d, 4H, **J**), 2.95-2.73 (d, 8H, **I**), 2.17 (s, 6H, **H**), 1.61 (s, 6H, **E**), 1.37 (s, 3H, **G**) Impurities: 5.45, 1.3, 0.86

HR-CMS-MS (233 K): calcd. for $C_{24}H_{36}N_4Ni^{2+}$ $[M\text{-}2SbF_6]^+$ 219.1141; exp 219.1120.

UV-vis(233 K): λ_{max} = 470 nm (ε = 1200 $M^{-1}cm^{-1}$)

5. NMR spectra for [(PyNMe$_3$)Ni(cycloneophyl)] complexes

5.1. NMR characterization of 2

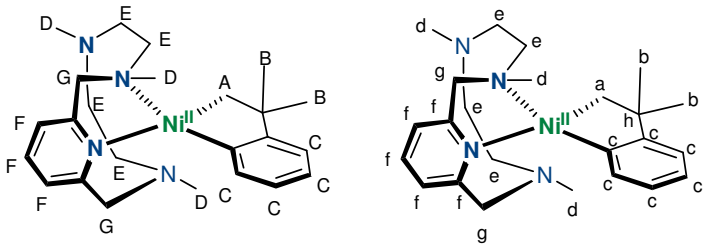

Scheme S7. ^{1}H NMR (left) and ^{13}C NMR (right) assignations for **2**.

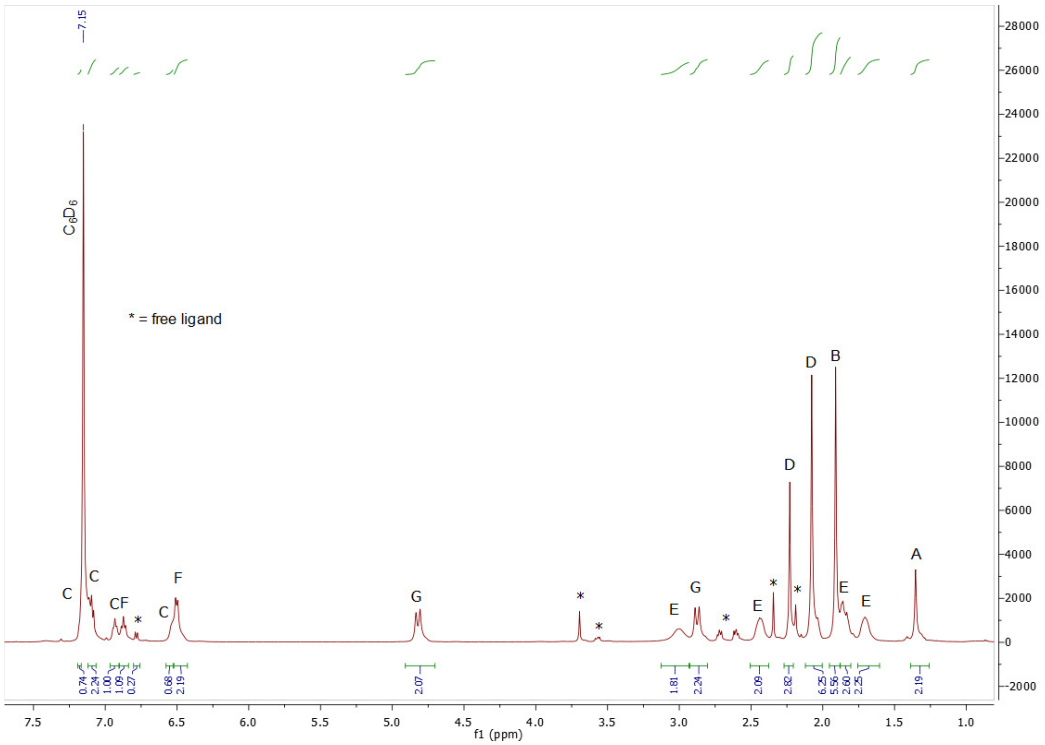

Figure S2. ^{1}H NMR (500 MHz, C_6D_6, 298 K) spectrum of **2** (* corresponds to free ligand peaks).

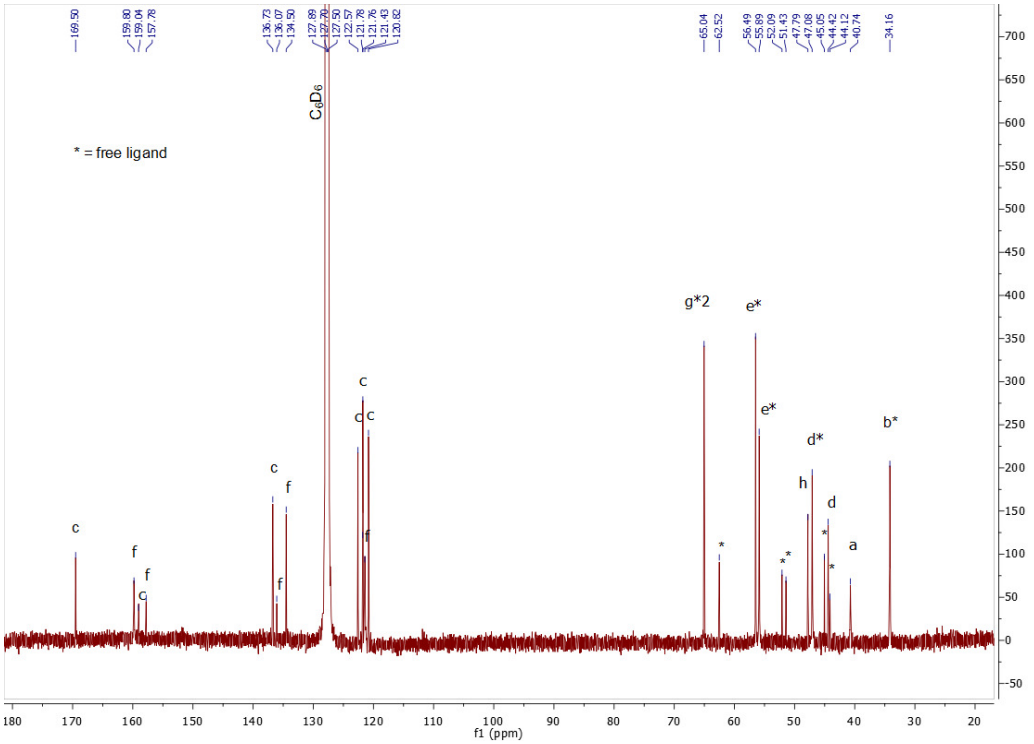

Figure S3. ^{13}C NMR (500 MHz, C_6D_6, 298 K) spectrum of **2** (* corresponds to free ligand peaks).

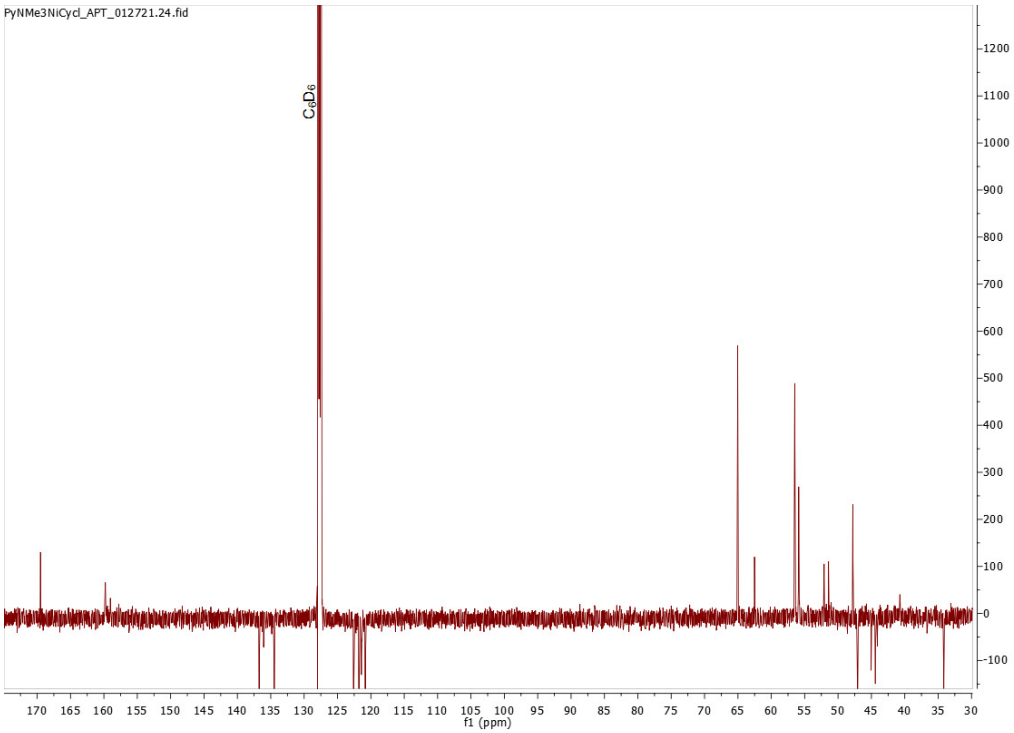

Figure S4. ^{13}C APT (500 MHz, C_6D_6, 298 K) spectrum of **2**.

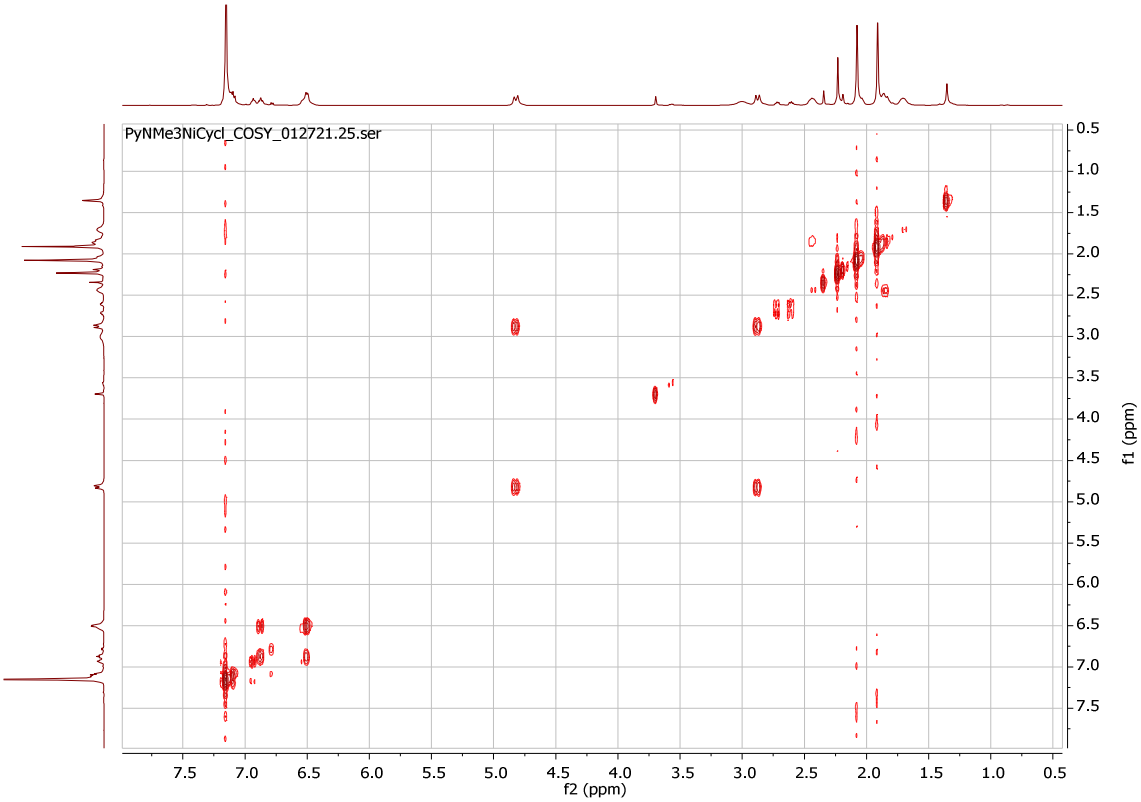

Figure S5. ^{1}H-^{1}H COSY NMR (500 MHz, C_6D_6, 298 K) spectrum of **2**.

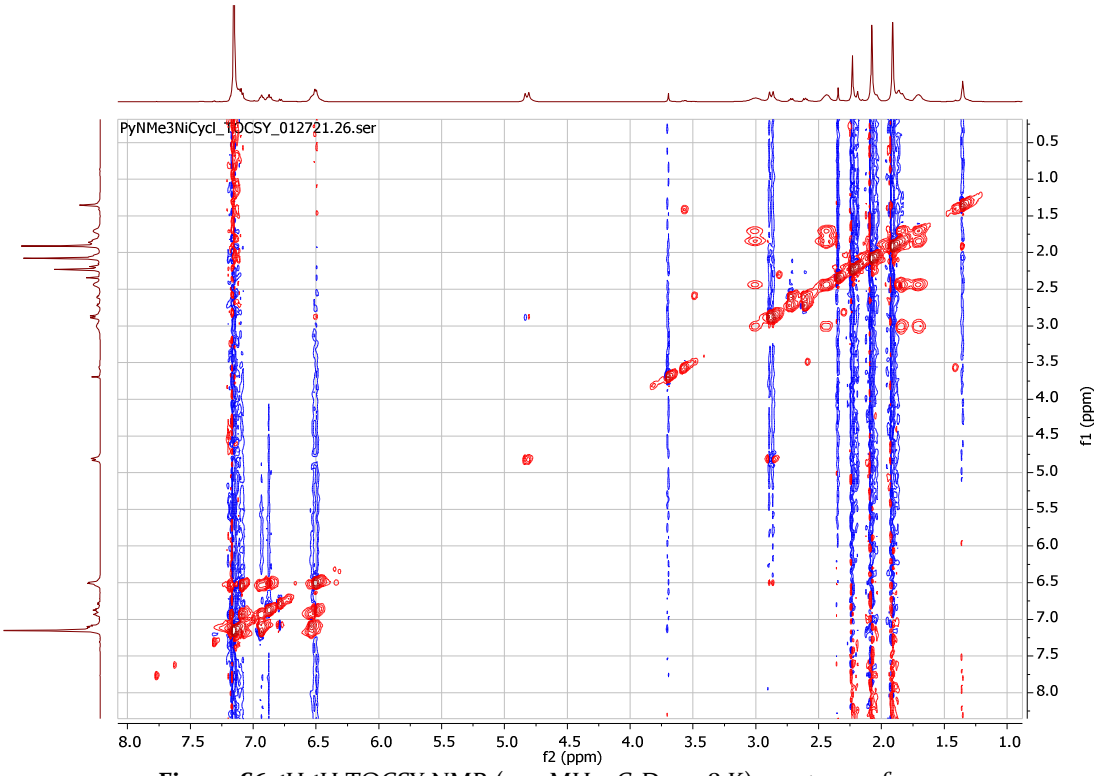

Figure S6. ^{1}H-^{1}H TOCSY NMR (500 MHz, C_6D_6, 298 K) spectrum of **2**.

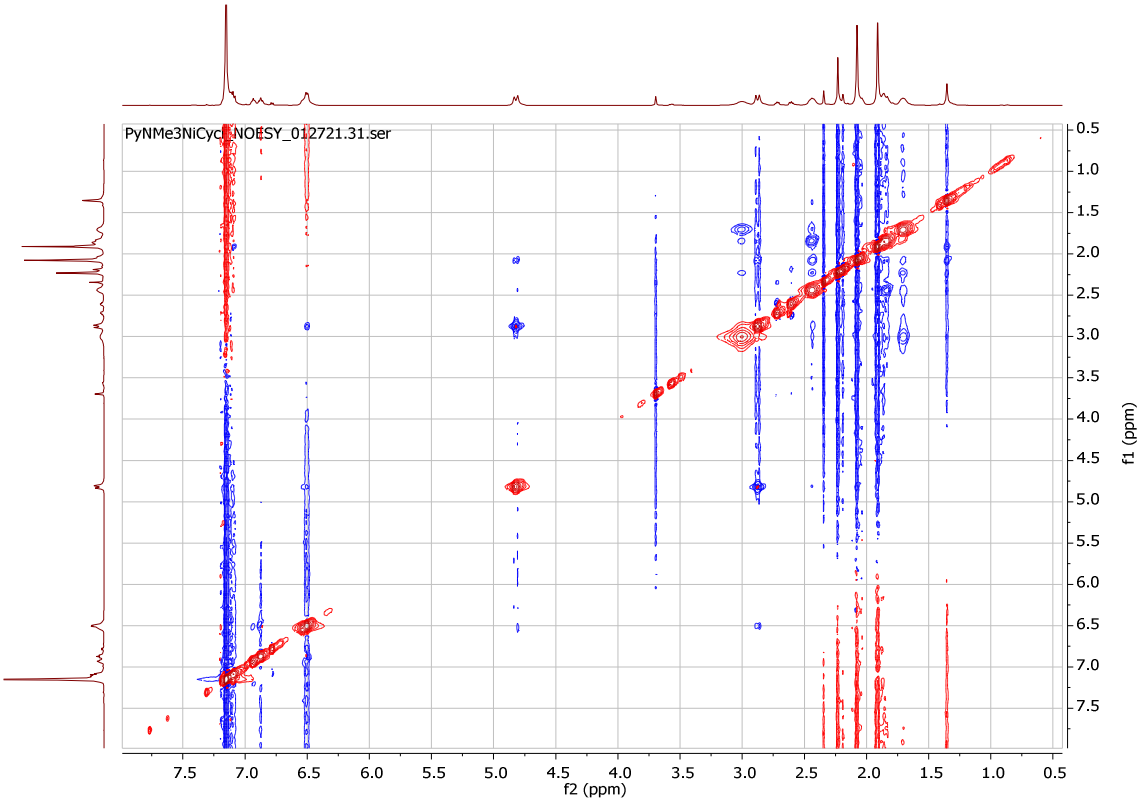

Figure S7. ^{1}H-^{1}H NOESY NMR (500 MHz, C_6D_6, 298 K) spectrum of **2**.

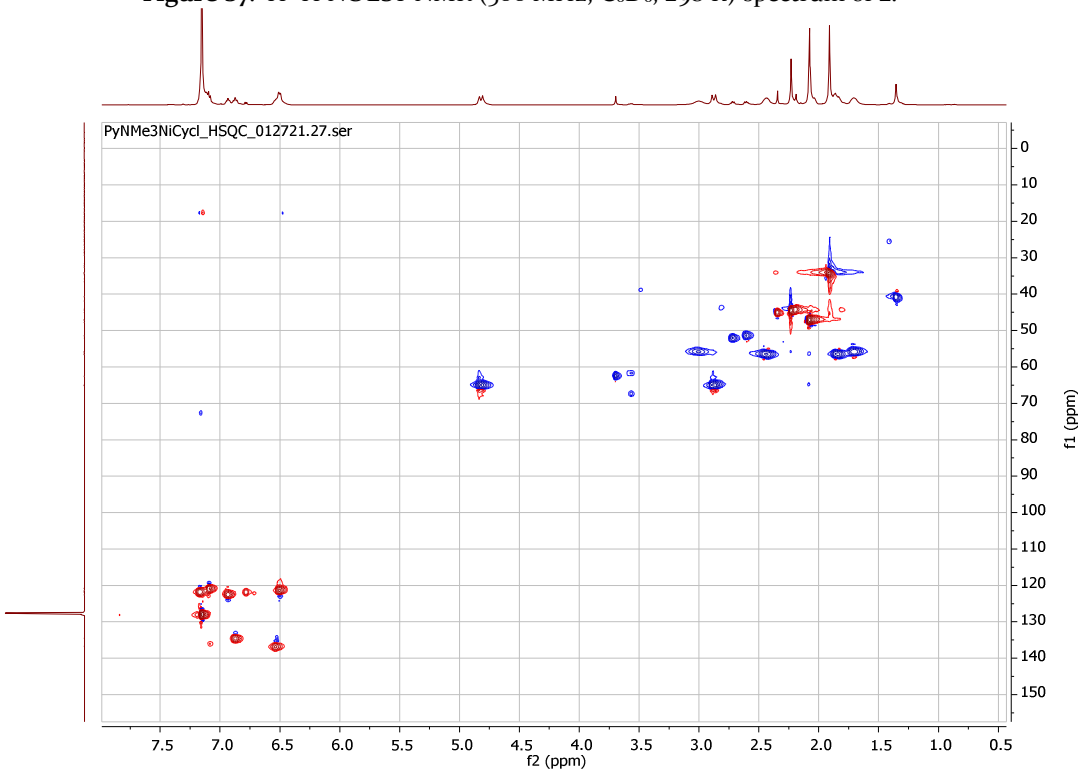

Figure S8. ^{1}H-^{13}C HSQC NMR (500 MHz, C_6D_6, 298 K) spectrum of **2**.

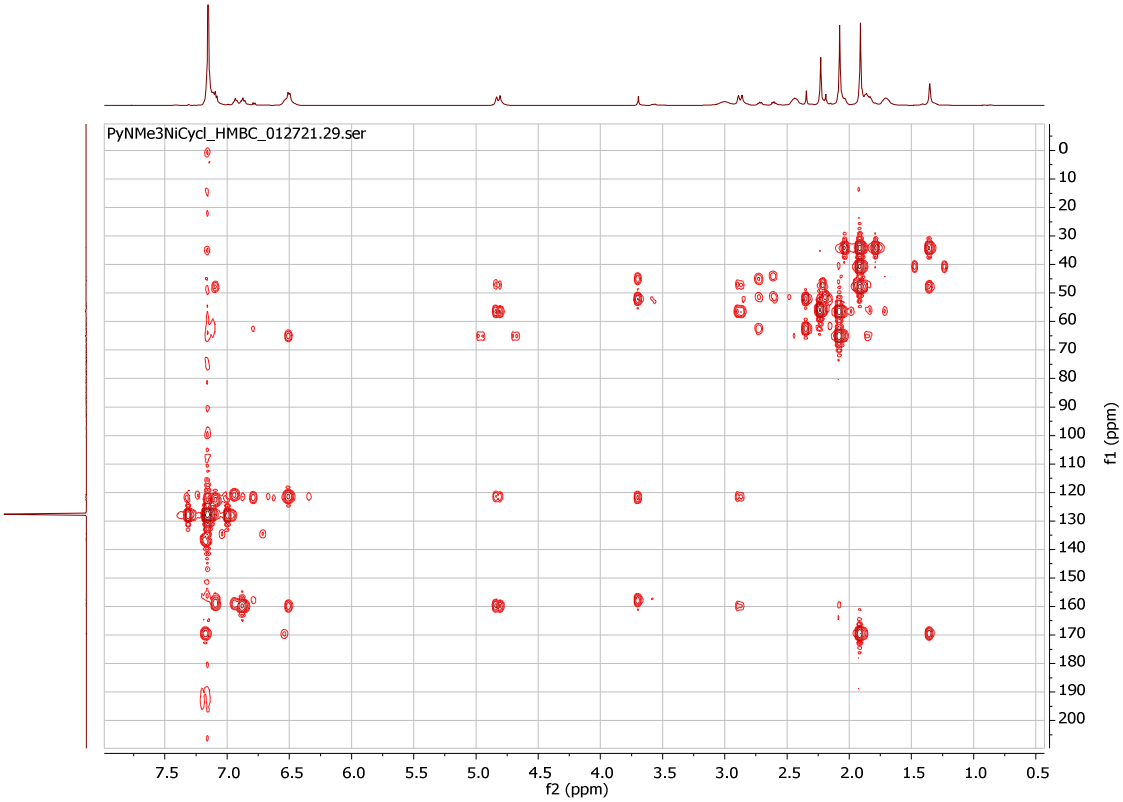

Figure S9. ^{1}H-^{13}C HMBC NMR (500 MHz, C_6D_6, 298 K) spectrum of **2**.

5.2. NMR comparison for complexes 2, 3 and 4

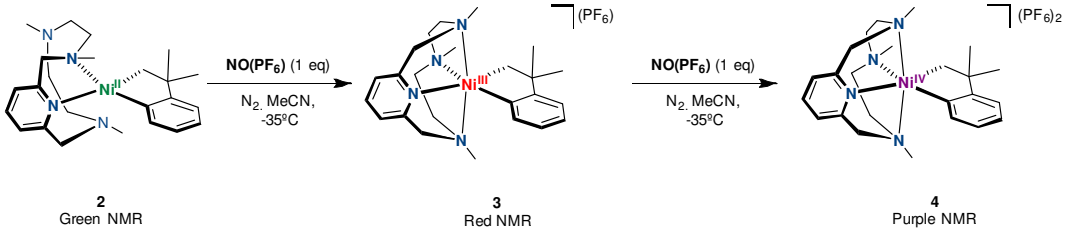

A stepwise $2e^-$ oxidation of $NOPF_6$ to **2** in a N_2-filled NMR tube. The addition of one equiv. oxidant converted the diamagnetic Ni^{II} complex (Stacked: Green Spectra) to a paramagnetic Ni^{III} species (**3**) (Stacked: Red Spectra). Upon the addition of the second equiv. of oxidant, the NMR signal became diamagnetic to form the proposed Ni^{IV} species (**4**) (Stacked: Purple Spectra). Broad Ni^{IV} peaks were observed, which are likely due to a small amount residual of Ni^{III}.

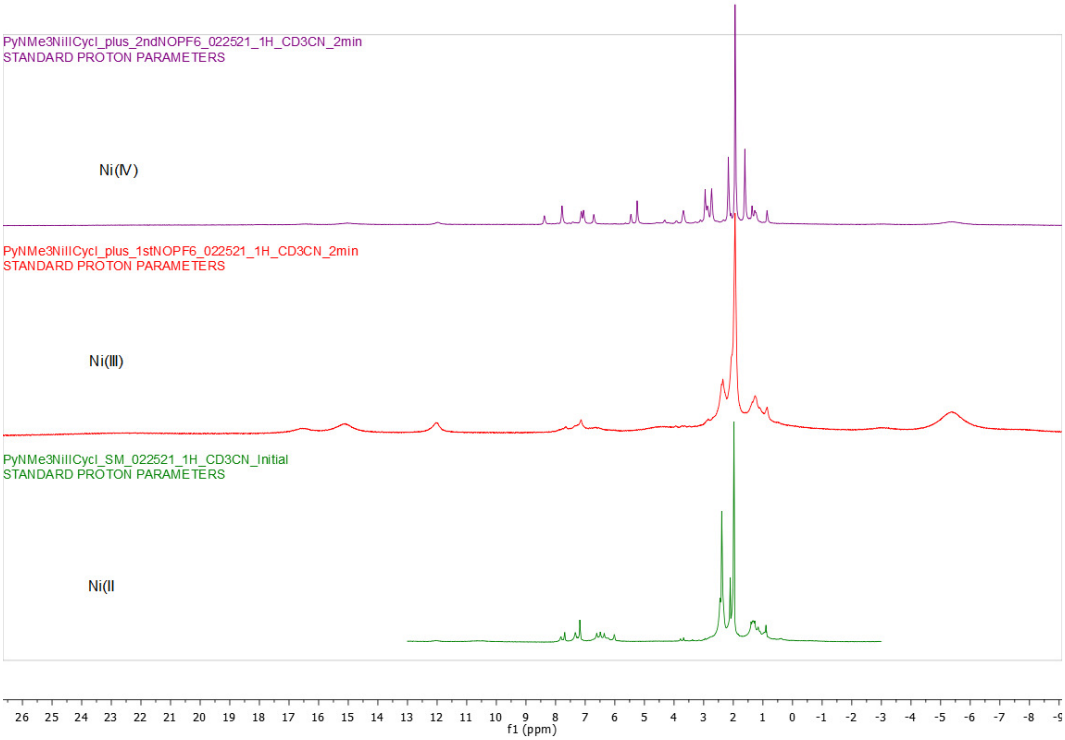

Figure S10. Stacked view of the ^{1}H NMR (500 MHz, CD_3CN, 238 K) spectra of $Ni^{II}/Ni^{III}/Ni^{IV}$ (complexes **2**/**3**/**4**, respectively).

5.3. NMR characterization of 4

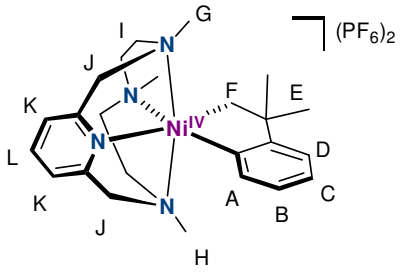

Scheme S8. ^{1}H NMR peak assignment for **4**.

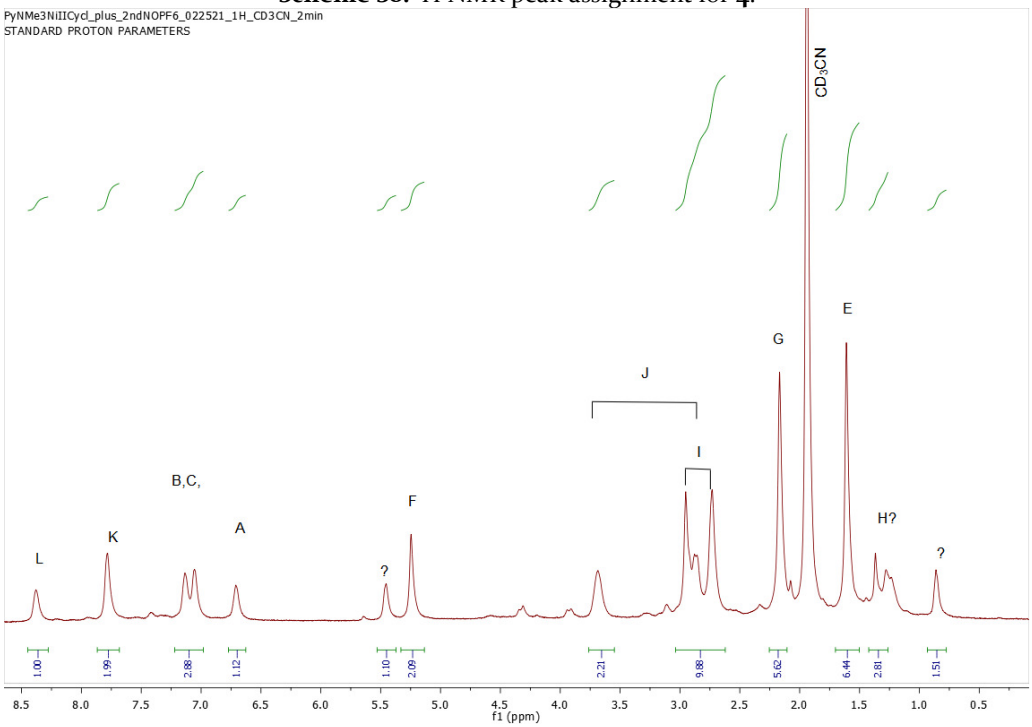

Figure S11. ^{1}H NMR (500 MHz, CD_3CN, 238 K) spectrum of **4**.

^{1}H NMR (500 MHz, CD_3CN, 238 K), δ (ppm): 8.38 (b, 1H, **L**), 7.78 (b, 2H, **K**), 7.14-7.05 (d, 3H, **B,C,D**), 6.70 (b, 1H, **A**), 5.25 (s, 2H, **F**), 3.70-2.86 (d, 4H, **J**), 2.95-2.73 (d, 8H, **I**), 2.17 (s, 6H, **H**), 1.61 (s, 6H, **E**), 1.37 (s, 3H, **G**). Unknown impurities: 5.45, 1.3, 0.86.

Peaks were assigned based on the previously isolated Ni^{IV} complexes $[^{Me}N4Ni(Cycloneophyl)]^{2+}$ and $[^{Me}TACNNi(Cycloneophyl)]^{2+}$.[4, 5]

6. Cyclic voltammogram (CV) of 2

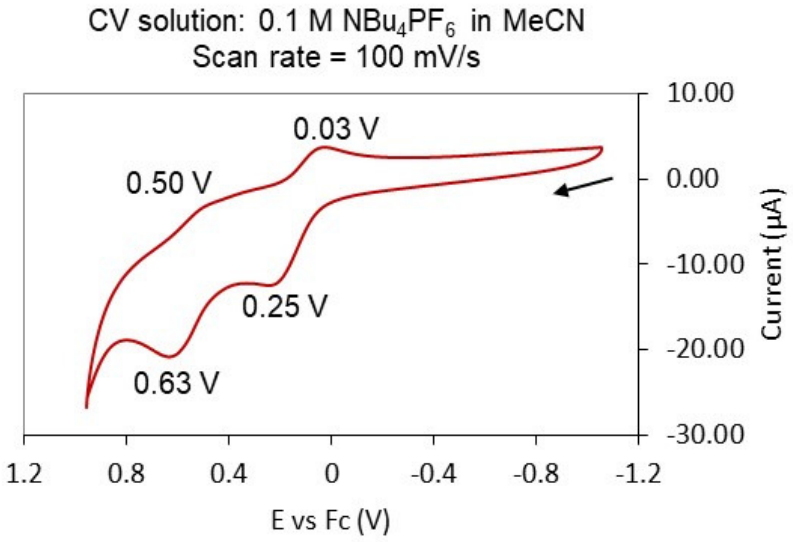

Figure S12. Cyclic voltammogram of **2** (Ag wire was used as reference electrode).

7. Simulation of EPR spectra of 3

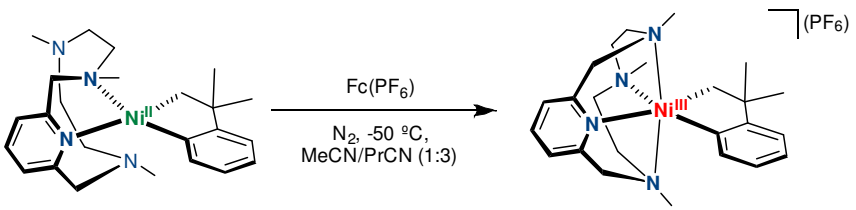

Scheme S9. Synthesis of **3** for EPR characterization.

In the glovebox, **2** (3.6 mg, 0.008 mmol) was dissolved in MeCN (100 µL) and cooled down to -50ºC. Then a cold suspension of $FcPF_6$ (2.7 mg, 0.008 mmol) in PrCN (300 µL) was layered over the complex solution. The resulting solution of 1:3 MeCN:PrCN was shaken for 5 seconds and then frozen in liquid nitrogen. After mixing, the dark blue colour of the oxidant suspension vanished immediately, and everything was in solution.

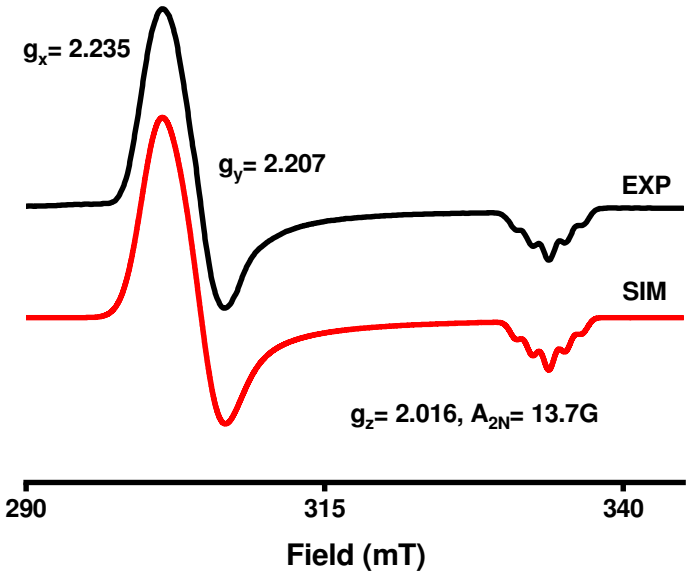

Figure S13. EPR spectra of **3** at low temperature (black line: experimental; red line: simulated).

Obs: The complex is stable at room temperature. Spectra of the initial complex (low temp, no warming up) and spectra of the complex after 30 min at room temperature remains the same.

8. UV/vis spectra of [(PyNMe$_3$)Ni(cycloneophyl)] complexes

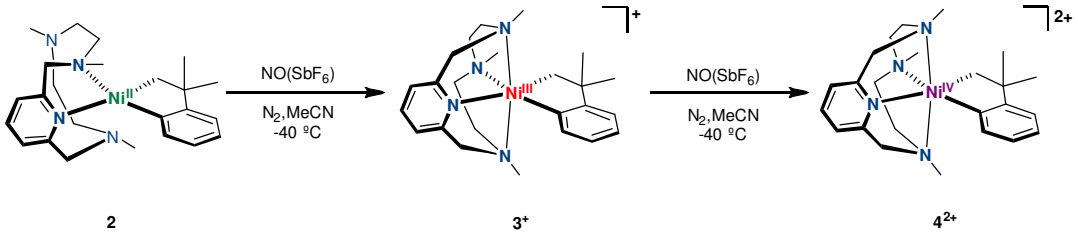

Scheme S10. Reaction scheme for the low-temperature UV/vis characterization of complexes **2**, **3** and **4**.

A UV-vis cell was charged with 2.2 ml of a 0.5 mM solution of **2** in anhydrous MeCN prepared in the glovebox. The quartz cell was capped with a septum, taken out of the glovebox, and placed in a Unisoku thermostated cell holder designed for low-temperature experiments at 233 K. Once the thermal equilibrium was reached, a UV/vis spectrum of the starting complex was recorded (green line). **2** exhibited a band at λ_{max} = 460 nm (ε = 880 $M^{-1}cm^{-1}$). After that, another equivalent of NO^+ was injected into the cell through the septum resulting in an immediate new spectrum corresponding to **3** (red line) which showed a band at λ_{max} = 510 nm (ε = 300 $M^{-1}cm^{-1}$). The nature of $\mathbf{3}^+$ was confirmed by HR-CMS-MS (calcd. for $C_{24}H_{36}N_4Ni^+$ [M-

$SbF_6]^+$ 438.2288; exp 438.2289). Finally, another equivalent of the same oxidant was added as before stated to the cuvette and instantly afforded a different spectrum corresponding to **4** (purple line) that presents a band at λ_{max} = 470 nm (ε = 1200 $M^{-1}cm^{-1}$) and a shoulder at 620 nm. Again, the identity of **4** was confirmed by HR-CMS-MS at 233 K (calcd. for $C_{24}H_{36}N_4Ni^{2+}$ $[M-2SbF_6]^{2+}$ 219.1141; exp 219.1120).

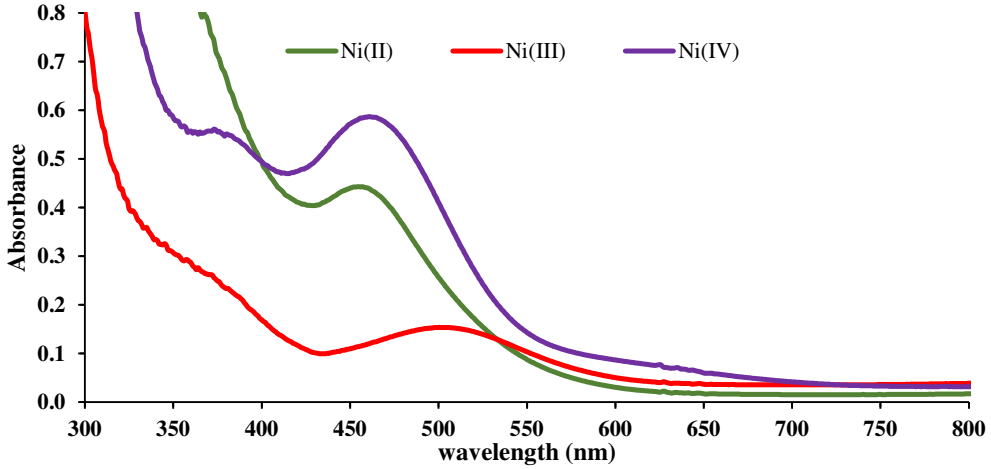

Figure S14. UV/Vis at -40 ºC, 0.5 mM solution of complexes **2**, **3** and **4** in MeCN.

9. Cryo-ESI-MS analysis of complexes 3 and 4

$[(PyNMe_3)Ni^{III}(cycl)]^+$, 3^+ (233 K)

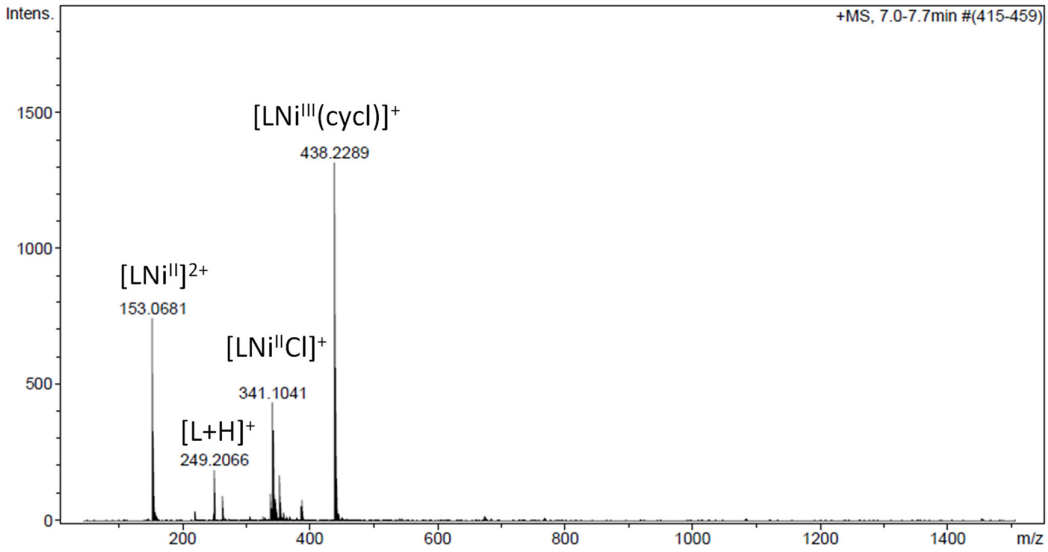

Figure S15. HR-cryo-MS of **3** at -40 ºC.

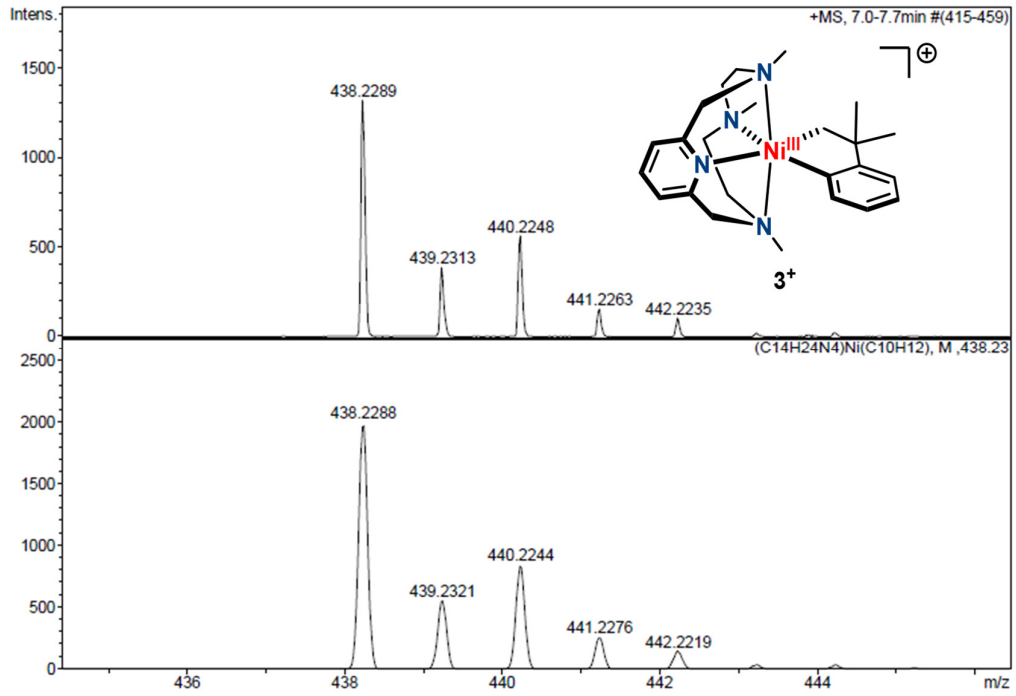

Figure S16. Zoom-in of the monocharged peak corresponding to $\mathbf{3}^{+}$.

$[(PyNMe_3)Ni^{IV}(cycl)]^{2+}$, $\mathbf{4}^{2+}$ (233 K)

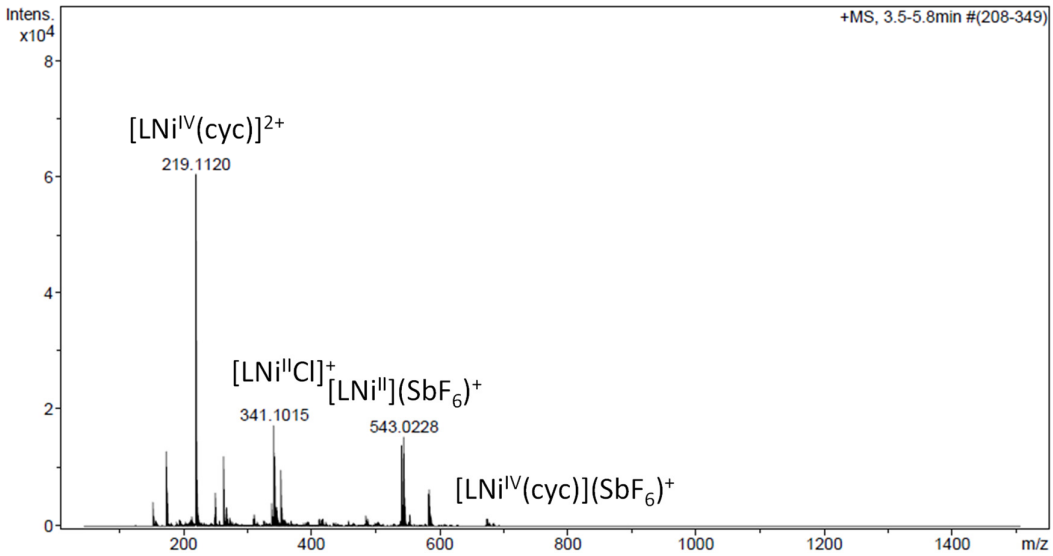

Figure S17. HR-cryo-MS of **4** at -40 ºC.

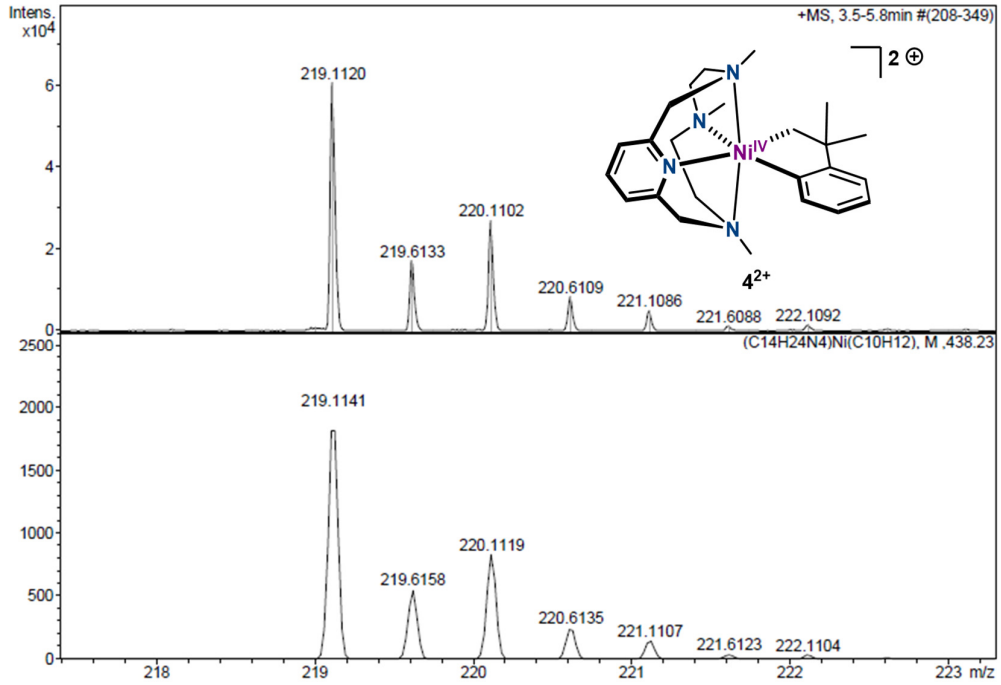

Figure S18. Zoom-in of the discharged peak corresponding to $\mathbf{4}^{2+}$.

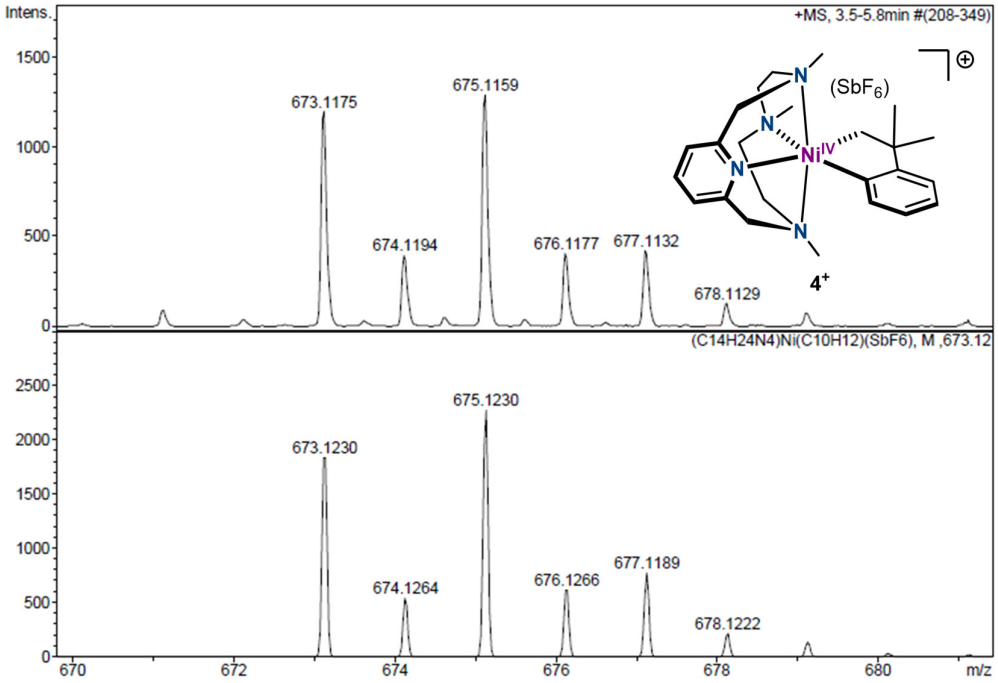

Figure S19. Zoom-in of the monocharged peak corresponding to $\mathbf{4}^{+}$.

10. Reactivity studies

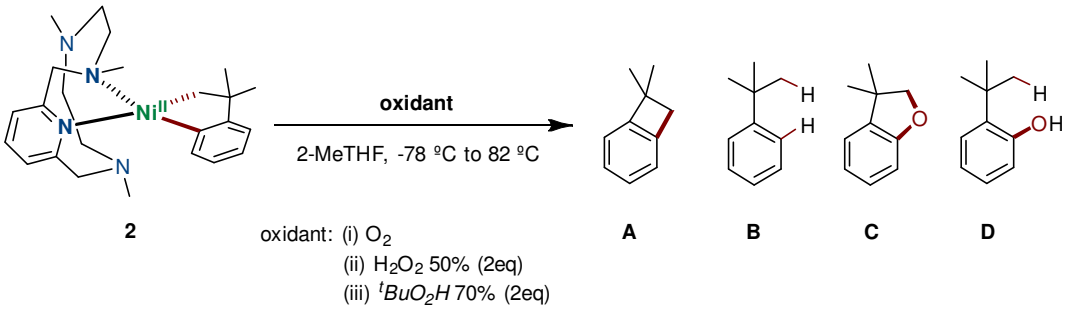

Scheme S11. Reactivity of **2** towards two-electron oxidants for the formation of C-C and C-O coupling products.

In a N_2-filled glovebox, **2** (2 mg) and 1.0 eq trimethoxybenzene were dissolved in 2 mL of 2-methyltetrahydrofuran. The mixture was allowed to cool down to -78 ºC, and then bubbled with dry oxygen for 30 seconds, or injected with 2.0 eq H_2O_2 (50 wt%) or $^tBuO_2H$ (70 wt%). After 15 minutes, aliquots were taken from the reaction mixture for GC-MS analysis and the solution was allowed to warm up to 22 ºC. After 1 hour at 22 ºC, aliquots were taken again, and the solution was heated to 82 ºC. After 24 and 48 hours at 82 ºC, aliquots were also taken.

For GC-MS analysis, the aliquots taken were added to 200µL of 14 wt% $HClO_4$ solution to completely protodemetallate the organic fragments. Then 1 mL saturated K_2CO_3 was added to the mixture to neutralize the solution, and the organic product was extracted twice with 0.5mL diethyl ether. The organic layer was dried over $MgSO_4$, filtered, and injected into GC-MS for analysis. The product yield was calibrated with a calibration curve against trimethoxybenzene.

Entry	Oxidant	Time	A (%)	B (%)	C (%)	D (%)	Sum(%)	C-O Sum (%)
1	O_2 (30s bubbling)	15min	55	0	0	0	55	0
2		15min + 1h	41	0	1	1	43	2
3		15min + 1h + 24h	41	2	4	1	48	5
4		15min + 1h + 48h	59	0	6	2	67	8
5	H_2O_2 2eq	15min	13	0	1	1	15	2
6		15min + 1h	9	1	5	2	17	7
7		15min + 1h + 24h	8	0	9	2	19	11
8		15min + 1h + 48h	9	1	11	2	23	13
9	$tBuO_2H$ 2eq	15min	5	0	1	1	7	2
10		15min + 1h	3	0	4	2	9	6
11		15min + 1h + 24h	3	0	7	2	12	9
12		15min + 1h + 48h	3	1	8	3	15	11

11. X-ray diffraction analysis

All X-ray structures are represented at 50% probability thermal ellipsoids and hydrogen atoms have been omitted for clarity.

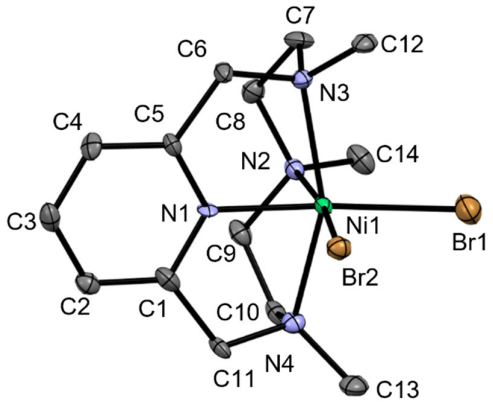

	1-Br (CCDC 2118410)
Chemical formula	$C_{14}H_{24}NiN_4Br_2$
Formula weight	466.90 g/mol
Temperature	100(2) K
Wavelength	0.71073
Crystal system	orthorhombic
Space group	$Pca2_1$
Unit cell dimensions	a = 14.5110(8) Å α = 90° b = 7.7903(5) Å β = 90° c = 30.1258(17) Å γ = 90°
Volume	3405.6(3) $Å^3$
Z, Density (calculated)	8, 1.821 g/cm^3
Absorption coefficient	5.831mm^{-1}
F(000)	1872
Crystal size	0.418 x 0.295 x 0.206 mm
Theta range for data collection	2.615 to 27.522°
Index ranges	-18≤h≤18, -10≤k≤6, -39≤l≤39
Reflections collected / Independent	32021/ 7798 [R(int) = 0.0466]
Completeness to Theta	99.9% (Theta = 25.242°)
Refinement method	Full-matrix least-squares on F^2
Data / restraints / parameters	7798 / 1 / 386
Goodness-of-fit on F^2	1.035
Final R indices	data R1 = 0.0461, wR2 = 0.11901 I>2σ(I) all data R1 = 0.0586, wR2 = 0.1259
Largest diff. peak and hole	and e$Å^{-3}$ 1.286 and -1.612 e.$Å^{-3}$

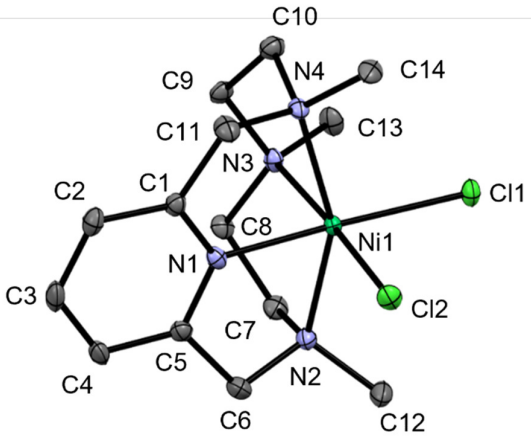

	1-Cl (CCDC 2118413)
Chemical formula	$C_{14}H_{24}NiN_4Cl_2$
Formula weight	377.98 g/mol
Temperature	100(2) K
Wavelength	0.71073
Crystal system	orthorhombic
Space group	$Pca2_1$
Unit cell dimensions	a = 25.5261(8) Å α = 90° b = 7.5526(2) Å β = 90° c = 34.2402(12) Å γ = 90°
Volume	6601.1(4) $Å^3$
Z, Density (calculated)	16, 1.521 g/cm^3
Absorption coefficient	1.498mm^{-1}
F(000)	3168
Crystal size	0.541 x 0.294 x 0.107 mm
Theta range for data collection	1.189 to 32.656°
Index ranges	-38≤h≤38, -5≤k≤11, -51≤l≤51
Reflections collected / Independent	24015/ 18871 [R(int) = 0.0447]
Completeness to Theta	99.9% (Theta = 25.242°)
Refinement method	Full-matrix least-squares on F^2
Data / restraints / parameters	7798 / 1 /770
Goodness-of-fit on F^2	1.012
Final R indices	data R1 = 0.0447, wR2 = 0.0741 I>2σ(I) all data R1 = 0.0671, wR2 = 0.0811
Largest diff. peak and hole	and $eÅ^{-3}$ 0.549 and -0.660 e.$Å^{-3}$

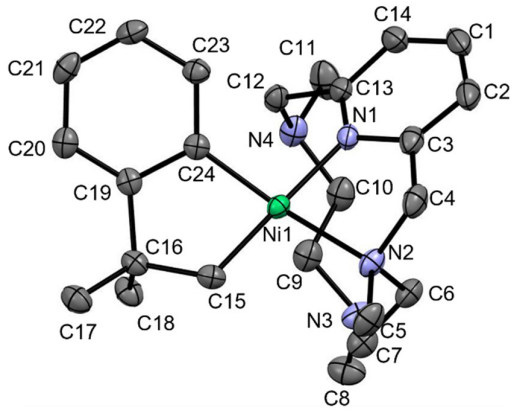

	2 (CCDC 2118411)
Chemical formula	$C_{24}H_{36}NiN_4$
Formula weight	439.27 g/mol
Temperature	100(2) K
Wavelength	0.71073
Crystal system	orthorhombic
Space group	$P2_12_12_1$
Unit cell dimensions	a = 10.3930(4) Å α = 90° b = 13.3946(5) Å β = 90° c = 15.9835(6) Å γ = 90°
Volume	2225.06(15)Å^3
Z, Density (calculated)	4, g/cm^3
Absorption coefficient	0.889 mm^{-1}
F(000)	984.0
Crystal size	0.446 × 0.297 × 0.227 mm
Theta range for data collection	4.674 to 56.588 °
Index ranges	-13 ≤ h ≤ 13-16 ≤ k ≤ 17-21 ≤ l ≤ 21
Reflections collected / Independent	62710/ 5516 [R_{int} = 0.0344, R_{sigma} = 0.0164]
Completeness to Theta	1.77/1.00 (Theta = 28.294 º)
Refinement method	Solved with the ShelXT structure solution program using Intrinsic Phasing and refined with the XL refinement package using Least Squares minimization.
Data / restraints / parameters	5516/0/267
Goodness-of-fit on F²	1.123
Final R indices	data R1 = 0.0249, wR2 = 0.0641 I>2σ(I) all data R1 = 0.0259, wR2 = 0.0647
Largest diff. peak and hole	and eÅ^{-3} 0.57/-0.53

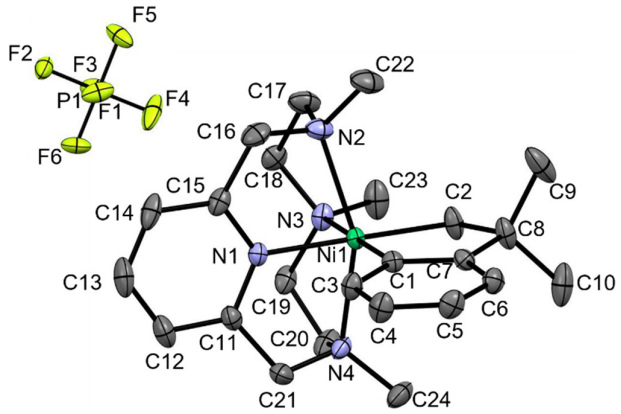

	3 (CCDC 2118412)
Chemical formula	$C_{24}H_{36}NiN_4PF_6$
Formula weight	584. 25 g/mol
Temperature	100(2) K
Wavelength	0.71073
Crystal system	monoclinic
Space group	$P2_1/n$
Unit cell dimensions	a = 8.4822(2) Å α = 90° b = 10.1578(2) Å β = 97.0100(10) ° c = 29.7277(6) Å γ = 90°
Volume	2542.21(9) $Å^3$
Z, Density (calculated)	4, g/cm^3
Absorption coefficient	0.891 mm^{-1}
F(000)	1220.0
Crystal size	0.201 × 0.113 × 0.079 mm
Theta range for data collection	4.24 to 56.58°
Index ranges	-11 ≤ h ≤ 11-13 ≤ k ≤ 13-39 ≤ l ≤ 39
Reflections collected / Independent	83724/ 6326 [R_{int} = 0.0351, R_{sigma} = 0.0149]
Completeness to Theta	0.999% (Theta =28.290 º)
Refinement method	Solved with the ShelXT structure solution program using Intrinsic Phasing and refined with the XL refinement package using Least Squares minimization.
Data / restraints / parameters	6326/0/330
Goodness-of-fit on F^2	1.039
Final R indices	data R_1 = 0.0283, wR_2 = 0.0691 I>2σ(I) all data R_1 = 0.0315, wR_2 = 0.0716
Largest diff. peak and hole	and $eÅ^{-3}$ 0.50/-0.44

12. References

1. C. Magallón, J. Serrano-Plana, S. Roldán-Gómez, X. Ribas, M. Costas and A. Company, Preparation of a coordinatively saturated μ-η2:η2-peroxodicopper(II) compound, *Inorg. Chim. Acta*, 2018, **481**, 166-170.
2. J. Serrano-Plana, W. N. Oloo, L. Acosta-Rueda, K. K. Meier, B. Verdejo, E. García-España, M. G. Basallote, E. Münck, L. Que, A. Company and M. Costas, Trapping a Highly Reactive Nonheme Iron Intermediate That Oxygenates Strong C—H Bonds with Stereoretention, *J. Am.Chem Soc.* 2015, **137**, 15833-15842.
3. J. Cámpora, M. a. del Mar Conejo, K. Mereiter, P. Palma, C. Pérez, M. L. Reyes and C. Ruiz, Synthesis of dialkyl, diaryl and metallacyclic complexes of Ni and Pd containing pyridine, α-diimines and other nitrogen ligands: Crystal structures of the complexes cis-NiR2py2 (R=benzyl, mesityl), *J. Organomet. Chem.*, 2003, **683**, 220-239.
4. J. W. Schultz, K. Fuchigami, B. Zheng, N. P. Rath and L. M. Mirica, Isolated Organometallic Nickel(III) and Nickel(IV) Complexes Relevant to Carbon–Carbon Bond Formation Reactions, *J. Am.Chem Soc.* 2016, **138**, 12928-12934.
5. M. B. Watson, N. P. Rath and L. M. Mirica, Oxidative C–C Bond Formation Reactivity of Organometallic Ni(II), Ni(III), and Ni(IV) Complexes, *J. Am.Chem Soc.* 2017, **139**, 35-38.